VOLUME 2, 2018
DOI: 10.31058/j.am.2018.25004

Nuclear Technique (PAT) Challenge (XRD & HV) Techniques for Probing Properties of Material Science (Aluminum Alloy)

Emad A. Badawi[1*], M. A. Abdel-Rahman[1], S. A. Aly[1], H. Ibrahim[1], M. Abdel-Rahman[1]

[1] Physics Department, Faculty of Science, Minia University, Egypt

Email Address

emad.badawi@mu.edu.eg (Emad A. Badawi), m_abdelrahman@mu.edu.eg (M. Abdel-Rahman)
[*]Correspondence: emad.badawi@mu.edu.eg

Received: 15 August 2018**; Accepted:** 28 October 2018**; Published:** 3 Decembre 2018

Abstract:

This work aims to study the effect of deformation on the natural aging of the heat treatable 6063Al-alloy. The influence of deformation on the aged samples was established by studying the aging behavior of 3 different aged samples; one non-deformed sample, and two samples deformed at 5% and 30% degree of deformation. This study was performed using the positron annihilation technique (PAT) as non-destructive nuclear technique, which clearly distinguished and described the aging behavior at different degrees of deformation. The effect of deformation on the natural aged 6063 Al-alloy samples was also studied by Vickers micro-hardness test. X-Ray Diffraction (XRD) measurements and analysis using Materials Analysis Using Diffraction (MAUD) program helped in detecting the crystallite size, micro-strain, lattice parameter, and dislocation density as a function of the natural aging time for the three different samples.

Keywords:

Positron Annihilation Lifetime, 6063 Al Alloy, XRD, MAUD Program, Crystallite Size, Micro-Strain, Lattice Parameter, Dislocation Density, Natural Aging, Deformation, Heat Treatable Alloys

1. Introduction

Aluminium and its alloys are broadly used in various applications for their outstanding properties; such as being lightweight, having good electrical and mechanical properties, etc. The 6xxx-group contains magnesium and silicon as major addition elements. These multiphase alloys belong to the group of commercial aluminium alloys, in which relative volume; chemical composition and morphology of structural constituents exert significant influence on their useful properties [1,2,3,4,5]. 6063 Al-alloys are used in architectural fabrication, making window and door frames, pipe, tubing, and furniture. The age hardening process of Al-alloys has three steps, solution treatment, is the first step in the precipitation hardening process where the alloy is heated above the solves temperature. Quenching the alloy is the second step of the process; it is the sudden

chilling of the metal in oil or water. The structure and the distribution of the alloying constituents that existed at the temperature just prior to cooling are frozen into the metal by quenching. Aging at room temperature is the third step of the process which is called natural aging [6]. One significant technique for improving the mechanical properties of Al-alloys is compression or cold work. Cold work (compression) is an important method that produces dislocations mainly used to improve the mechanical properties of Al-alloys [7]. When compression is applied to a metal or alloy, it results in a change in the material's shape, which is referred to as plastic deformation. Plastic deformation is defined as the change in irreversible permanent shape after removing the applied load [8].

The combination of plastic deformation and aging processes were studied heavily in many researches [9,10,11]. In this paper, the combination of plastic deformation and natural aging were studied using Positron annihilation lifetime Spectroscopy, Vickers hardness test, and X-ray diffraction. Positron annihilation lifetime Spectroscopy (PALS) is a main tool used in materials science to study the defect properties. The main advantages of this tool is that it is a very sensitive non-destructive nuclear technique, and it is capable of differentiating between various types of defects for example vacancies, dislocations, grain boundaries, voids, … etc. [12]. Vickers micro-hardness (HV) is another common method that is used in measuring the hardness of metals and alloys [13]. Thus, it can be easily used in detecting the impact of compression combined with aging in metals and alloys. X-ray diffraction (XRD) is usually used for phase identification and to study the crystal structure of metals and alloys. XRD is one of the trustable methods that are used in detecting the precipitation resulting from aging and plastic deformation processes [14].

2. Experimental procedure

2.1. Samples Preparation

6063Al-alloy samples, with the chemical composition shown in Table 1, were used in this study. After cutting and grinding the samples, they were annealed at 413℃ for 3 hours to remove the internal stresses and any other defects that were produced through the preparation process. All the annealed samples were heated to 522℃ for 1 hour then quenched in water at room temperature to start the natural aging process. One group of the samples to study the behavior of the natural aging without any deformation, two other groups were deformed at 5% and 30% to study the influence of the deformation on the behavior of the natural aging.

Table 1. *The chemical composition of 6063 Al-alloy.*

Alloy	Cu	Fe	Mg	Ti	Mn	Si	Cr	Zn	Other	Al
6063	0.1	0.35	0.45-0.9	0.1	0.1	0.2-0.6	0.1	0.1	0.25	97.5

2.2. Experimental techniques:

2.2.1. Positron annihilation lifetime technique (PALT):

The positron annihilation lifetime technique is a suitable defect characterization technique [15,16,17,18], in this study, the positron lifetime measurements were performed at room temperature using a fast-fast coincidence system. The time resolution of the system using a ^{60}Co source was approximately 342 ps. Positron lifetime spectrum was accumulated for a period of 2 hours using ^{22}Na source. For each spectrum about one

million coincidence counts were accumulated. Lifetime spectra were analyzed as two lifetime components using PATFIT program [19].

2.2.2. Vickers Micro-hardness test (HV)

The hardness measurements for the 3 groups were performed using Vickers hardness test. Hardness is the property of a material that enables it to resist plastic deformation, usually by penetration. However, the term hardness may also refer to resistance to bending, scratching, abrasion or cutting. The Vickers hardness test method consists of indenting the test material with a diamond indenter, in the form of a right pyramid with a square base and an angle of 136 degrees between opposite faces subjected to a load of 1 to 100 kgf. The applied load used during Vickers hardness experiment is 4.9 N. The full load is normally applied for 10 to 15 seconds. The two diagonals of the indentation left in the surface of the material after removal of the load are measured using a microscope and their average calculated. The area of the sloping surface of the indentation is calculated. The Vickers hardness is calculated by dividing the applied load by the square the area of indentation [20].

$$HV = \frac{2Fsin\frac{136}{2}}{d^2} = 1.854\ \frac{F}{d^2} \quad (1)$$

Where F is the applied load in kgf, d is the arithmetic mean of the two diagonals in mm HV is the Vickers hardness

2.2.3. X-ray Diffraction (XRD)

A JEOL X-ray diffractometer (XRD) (Model JSDX-60PA) equipped with a Cukα-radiation (λ=0.145184nm) was used. X-ray source was operated at 40kv and 35mA. Continuous scanning was applied with a slow scanning rate (1o/min) and a small time constant (1sec). A range of 2θ (from 30 to 100 o) was scanned, so that the required diffraction peaks for phase identification could be detected. XRD measurements were performed for the three groups as a function of the natural aging time.

3. Results and Discussion

3.1. Positron Annihilation Lifetime

The effect of deformation on the aging behavior of age hardening 6063 Al-alloy through the positron mean lifetime measurements is depicted in Figure 1. The positron mean lifetime values were obtained at zero, 5% and 30% degrees of deformation. The measured positron mean lifetime values for the zero deformed sample has a linear behavior as a function of the aging time. With increasing the degree of deformation, the lifetime is increased. Maximum positron mean lifetime values were obtained at 30% degrees of deformation. An exponential decrease of the positron mean lifetime values were observed until stability is reached after around 200 and 350 hours for 5% and 30% deformations, respectively.

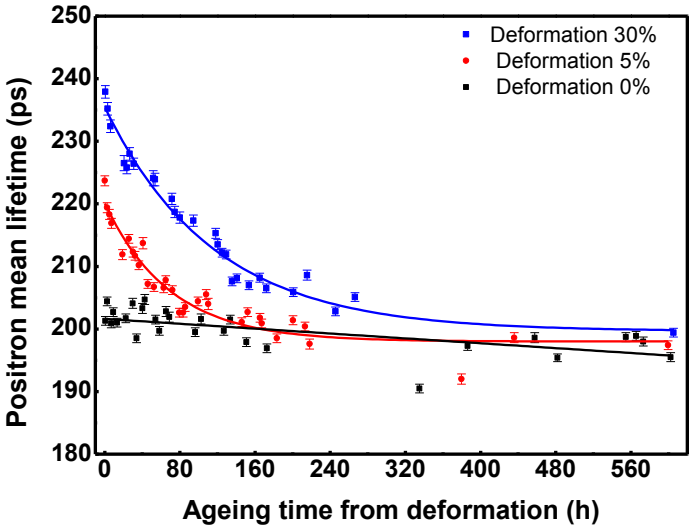

Figure 1. *The positron mean lifetime vs. aging time.*

3.2. Hardness Test

The Vickers hardness as a function of the aging time is shown in Figure 2. This figure reveals an increase in the sample hardness with increasing the degree of deformation. Vickers hardness numbers around 15, 20 and 22 HV was observed for the non-deformed, 5% and 30% degree of deformation respectively.

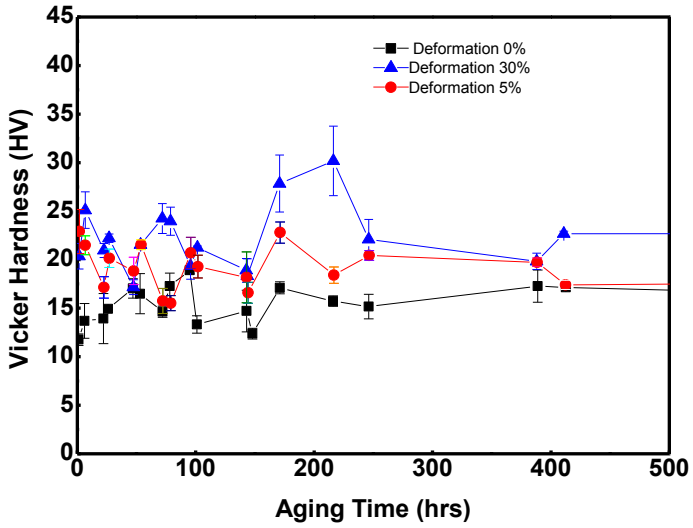

Figure 2. *The Vickers hardness vs. aging time.*

The value of the Hv for sample deformed at 30 % is higher than the sample deformed at 5 % which is also higher in values than non-deformed samples as shown in Figure 2 as a function of aging time. This also could be observed by the lifetime as shown in figure 5. It is around 15 HV (number) for the non-deformed sample, around 20 HV (number) for the NAD5%, and around 22 HV (number) for the NAD 30%. Hardness Test & Dislocation Density Behavior as a Function of Natural Aging Time. In the

hardness measurement, the used samples are the same as those used for the lifetime measurement (NA ONLY, NAD 5%, and NAD 30%).

3.3. X-Ray Diffraction

The X-ray powder diffraction data of the samples have been recorded in some days during natural aging. The main features of the diffraction patterns are the same, but only a considerable variation of the peak intensity is observed. The diffraction peaks at 2θ = 38.5, 44.8, 65.2, 78.1, and 82.3 are corresponding to the (111), (200), (220), (311), and (222) planes of the face centre cubic aluminum, respectively as confirmed by JCPDS X-ray powder file data. However, in all cases the intensities of (111) and (200) were high in comparison with other reflections, as shown in Figure 3.

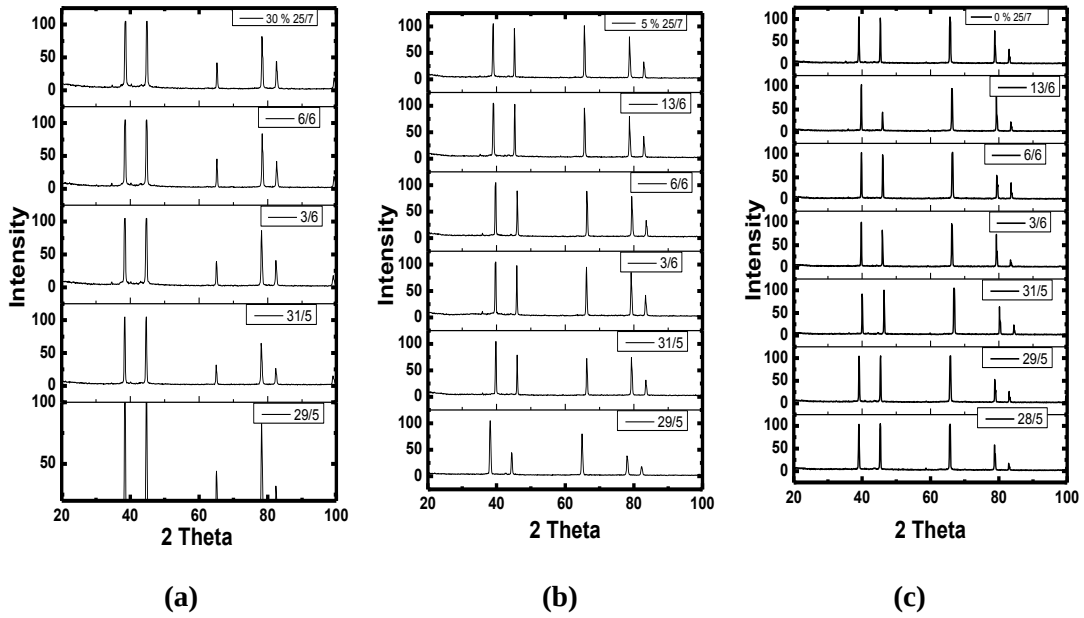

Figure 3. *XRD patterns for different 6063 Al-ally samples at (a) non-deformed, (b) 5 % and (c) 30 % degree of deformation.*

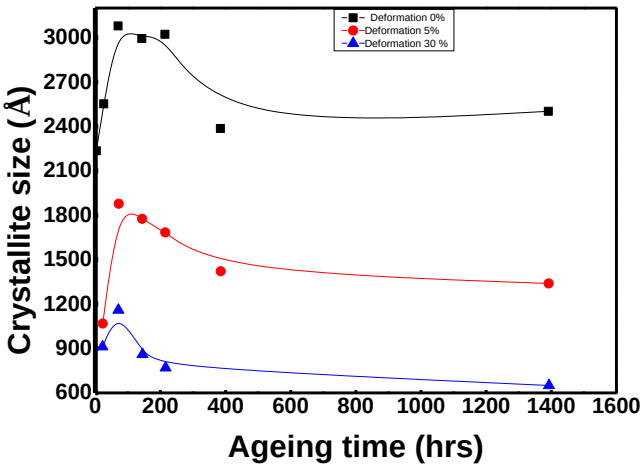

Figure 4. *Crystallite size vs. aging time.*

Figure 4 depicts the relation between the crystallite size and the aging time at zero, 5% and 30% degrees of deformation of 6063 Al-alloy. One can observe all over the aging time range (1400 hours) that the crystallite size is decreased with increasing the degree of deformation. The crystallite size decreases with increasing aging time up to 400 hours aging time at which the crystallite size approximately remaining constant for all deformed and non-deformed samples. Mean crystallite size of about 86, 177 and 300 nm was obtained for 30%, 5% and zero deformations, respectively at 145 hours of aging time. Figure 5 shows the relation between the micro-strain and aging time at zero, 5% and 30% degree of deformation of 6063 Al-alloy. We can observe that the micro-strain values increased with increasing the degree of deformation in contrast of the crystallite size, except for 5% deformed sample at the beginning of aging time. The 5% deformed sample shows micro-strain values higher than that of the 30% deformed sample just below 100 hours of aging time which might be referred to the effect macro-strain. The lattice parameter (Å) as a function of aging time for non-deformed, 5 % and 30 % of 6063 Al-alloy changes from 4.039 to 4.066 Å as observed from Figure 6.

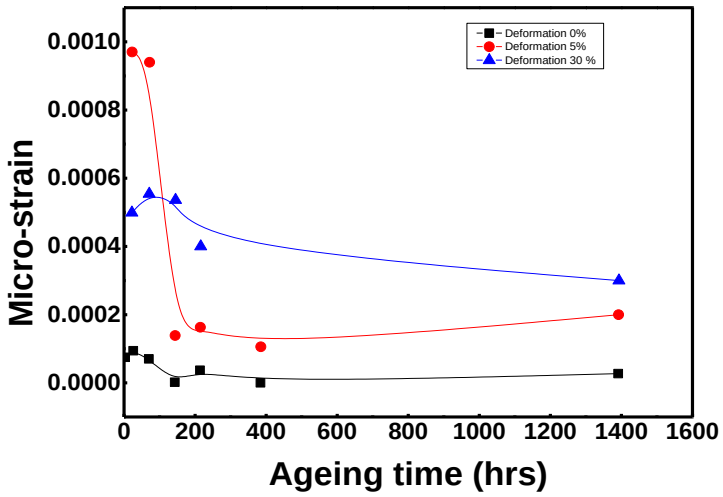

Figure 5. *Micro-strain vs. aging time.*

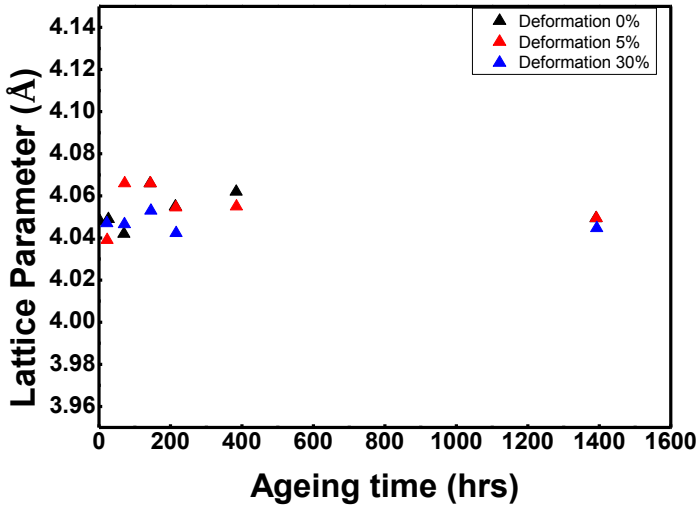

Figure 6. *Lattice parameter vs. aging time*

The dislocation density of all samples under investigation was determined by analyzing the XRD patterns via the Rietveld software materials analysis using (MAUD) [21]. In some recent studies [22,22,23,24,25,26], MAUD has been applied to characterize the microstructural parameters of different materials including the calculations of the lattice parameter, phase percentage, crystallite size and residual micro-strain. Details of method of analysis have been reported elsewhere [19,20,21,22]. The value of the dislocation density ρ (cm^{-2}) was calculated from the average values of the crystallite size D and micro-strain$\langle\varepsilon^2\rangle^{1/2}$ by [23]:

$$\rho = \frac{3\sqrt{2\pi}\,\langle\varepsilon^2\rangle^{1/2}}{Db} \tag{2}$$

where b is the Burgers vector (b = a/√2 for the fcc structure where a is the lattice parameter).

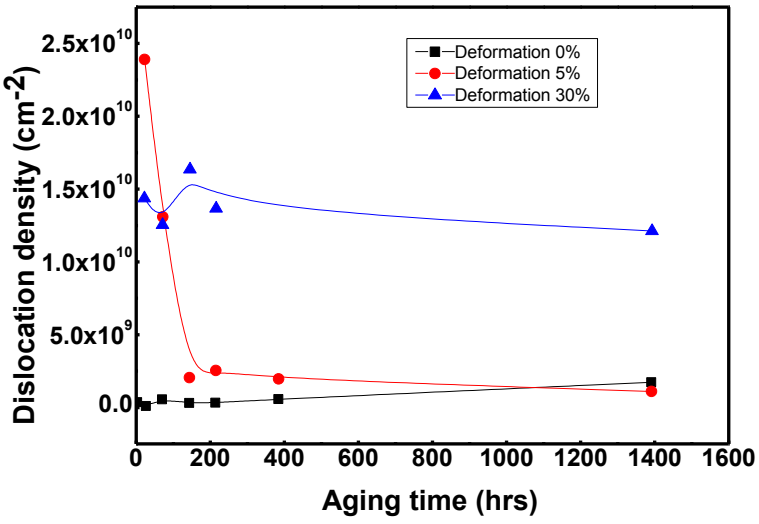

Figure 7. *Dislocation density vs. aging time.*

The dislocation density as a function of aging time for 6063 Al-alloy is shown in Figure 7. The dislocation density of the non-deformed sample changed linearly with aging time. Higher dislocation densities were obtained with increasing the degree of deformation. Micro-strain and dislocation density values shown in Figure 6 and Figure 7) show the same behavior all over the aging time range. In addition the 5% deformed sample shows micro-strain values higher than that of the 30% deformed sample just below 100 hours of aging time.

Table 2*. Shows the Intensity ratio of the first peak of the XRD pattern for 6063 Al-alloy.*

Sample 6063	Degree of deformation 0%	Degree of deformation 5%	Degree of deformation 30%
At Starting	0.994269(RO)	2.358108(PO)	1(RO)
At Final	1.028459(RO)	1.09384(RO)	1(RO)

At lower ageing time the preferred orientation (PO) (intensity ratio greater than 1) appeared at 5% thickness reduction as shown in table 2. The preferred orientation disappeared for zero and 30% degree of deformation at lower and higher aging time, in addition to 5 % deformation at higher aging time at which random orientation (RO) (intensity ration around 1) was observed. This means that at higher aging time the preferred orientation independent on reduction since the three samples gives the same intensity ratio around 1. Since at lower ageing time the micro-strain decreases with

degree of deformation, except sample with 5% deformation and at higher ageing time the micro-strain independent on deformation, hence the micro-strain depends on preferred orientation. The texture coefficient as a function of aging time for maximum intensity lines are shown in Figure 8 and Figure 9. There is agreement for the intensity ratio of the maximum lines with the behavior of micro-strain as shown in Figure 10.

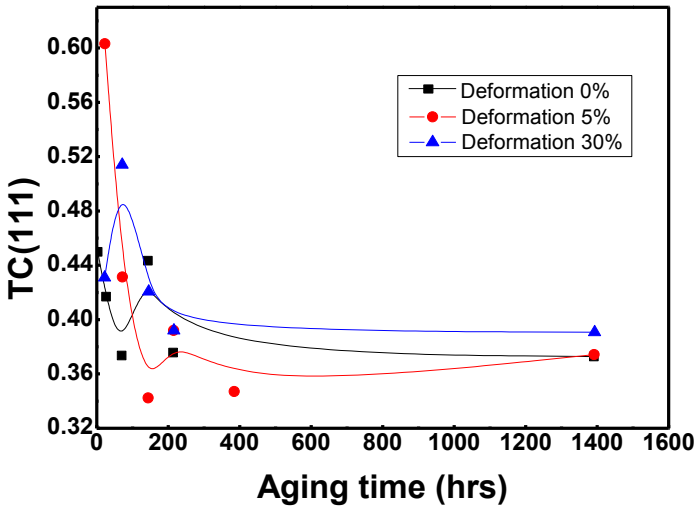

Figure 8. *The texture coefficient at (111) vs. ageing time.*

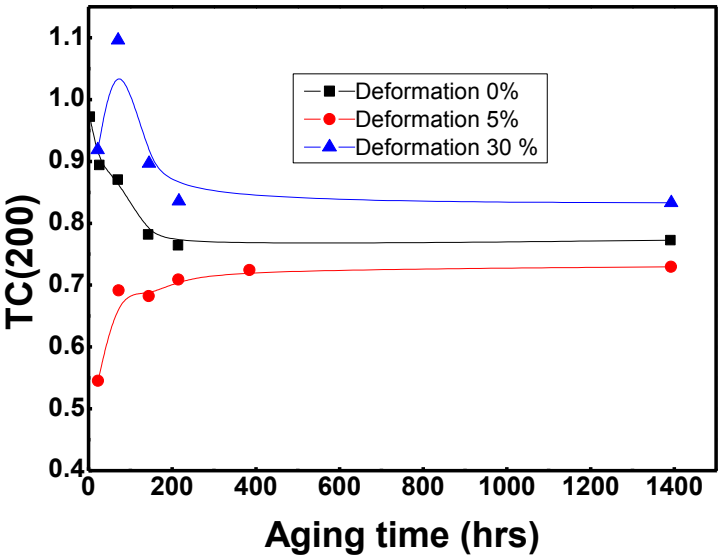

Figure 9. *The texture coefficient at (200) vs. ageing time.*

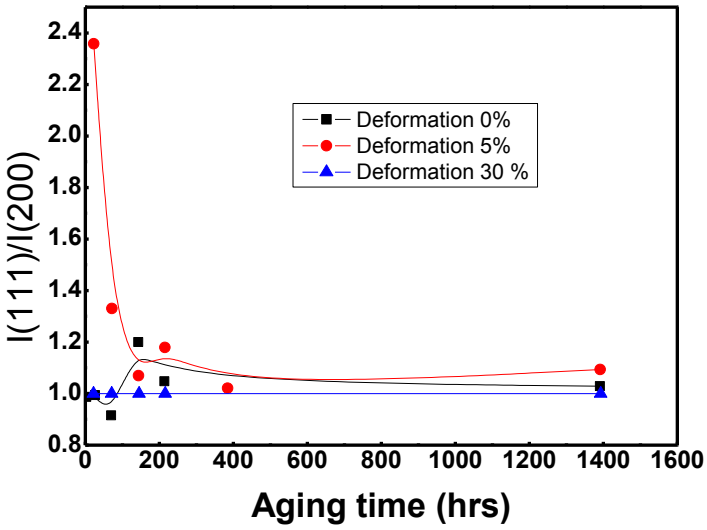

Figure 10. *The ratio of the I(111)/I(200) as a function of ageing time.*

4. Conclusions

According to the results and discussion the following items we can conclude:

I. The effect of natural aging on the lifetime and the crystallite size is not removed from the alloy with the time of aging up to 400 hours (about 16 days).

II. Micro-strain and dislocation density are higher as a function in the range of degree of deformation. They decrease as a function of aging time by the XRD parameter study. Lifetime decrease as a function of aging time by the positron lifetime spectroscopy study.

III. Only the binging degree of deformation at 5 % is higher (below 100 h aging) than (30 % degree of deformation) due to the effect of macro-strain is predominated than the micro-strain.

IV. The hardness value around 15 HV (number) for the non-deformed sample, around 20 HV (number) for the 5% degree of deformation, and around 22 HV (number) for the 30% degree of deformation.

V. There is a good correlation between XRD and lifetime measurements as a function of natural aging under different deformations.

VI. With higher aging time, the preferred orientation is independent on reduction since the three samples give the same intensity ratio.

Acknowledgement

Authors wish to great thank Professor M. A. Refat for his guide during the Materials Analysis Using Diffraction (MAUD) program of the X-Ray Diffraction analysis.

References

[1] Kuijpers NCW; Kool WH, Koenis PTG; Nilsen KE; Todd I; Van der Zwaag S. Assessment of different techniques for quantification of α-Al (FeMn) Si and β-AlFeSi intermetallics in AA 6xxx alloys. Materials Characterization, 2002, 49(5), 409-420.

[2] Polmear IJ. Light alloys-Metallurgy of the light metals//((Book)). London and New York, Edward Arnold, 1989, 288. 1989.

[3] Zajac S; Bengtsson B; Jonsson Ch. Influence of cooling after homogenization and reheating to extrusion on extrudability and final properties of AA 6063 and AA 6082 alloys. *Materials Science Forum,* 2002, 396-402:399-404.

[4] Meredith MW; Worth J; Hamerton R. Intermetallic phase selection during solidification of Al-Fe-Si (-Mg) alloys. *Materials Science Forum,* 2002, 396, 107-112.

[5] Warmuzek M; Sieniawski J; Gazda A; Mrówka G. Analysis of phase formation in AlFeMnSi alloy with variable content of Fe and Mn transition elements. *Materials Engineering,* 2003, 137, 821-4.

[6] Milkereit B; Giersberg L; Kessler O; Schick C. Isothermal time-temperature-precipitation diagram for an aluminum alloy 6005A by in situ DSC experiments. *Materials,* 2014, 28, 7(4), 2631-49.

[7] Abdel-Rahman M.; Salah Mohammed; Ibrahim Alaa M.; Badawi Emad A. Comparative techniques to investigate plastically deformed 5754 Al-alloy. *Modern Physics Letter B,* 2017, 31(28), 1750255-8

[8] Mostafa KM; Baerdemaeker JD; Calvillo PR; Caenegem NV; Houbaert Y; Segers D. A study of defects in iron based alloys by positron annihilation techniques. *Acta Physica Polonica-Series A General Physics,* 2008, 113(5), 1471-8.

[9] Marcinkowski MJ; Szirmae A; Fisher R. Effect of 500 Degrees C Aging on Deformation Behavior of Iron-Chromium Alloy. *Transactions of the Metallurgical Society of AIME,* 1964, 230(4), 676.

[10] Shekhter A; Aaronson HI; Miller MR; Ringer SP; Pereloma EV. Effect of aging and deformation on the microstructure and properties of Fe-Ni-Ti maraging steel. *Metallurgical and Materials Transactions A,* 2004, 35(3), 973-83.

[11] Raeder CH; Felton LE; Tanzi VA; Knorr DB. The effect of aging on microstructure, room temperature deformation, and fracture of Sn-Bi/Cu solder joints. *Journal of Electronic Materials,* 1994, 23(7), 611-7.

[12] Dupasquier A; Mills Jr AP, editors. Positron spectroscopy of solids. IOS press; 1995.

[13] Herrmann K, editor. Hardness testing: principles and applications. ASM International; 2011.

[14] Kaneko K; Hata T; Tokunaga T; Horita Z. Fabrication and characterization of supersaturated Al-Mg alloys by severe plastic deformation and their mechanical properties. *Materials transactions,* 2009, 50(1), 76-81.

[15] Krause-Rehberg R; Leipner HS. Positron annihilation in semiconductors: defect studies. Springer Science & Business Media; 1999.

[16] Tuomisto F; Ranki V; Saarinen K; Look DC. Evidence of the Zn vacancy acting as the dominant acceptor in n-type ZnO. *Physical Review Letters,* 2003, 91(20), 205502.

[17] Dutta S; Chakrabarti M; Chattopadhyay S; Jana D; Sanyal D; Sarkar A. Defect dynamics in annealed ZnO by positron annihilation spectroscopy. *Journal of applied physics,* 2005, 98(5), 053513.

[18] Chakrabarti M; Bhowmick D; Sarkar A; Chattopadhyay S; Dechoudhury S; Sanyal D; Chakrabarti A. Doppler broadening measurements of the electron-positron annihilation radiation in nanocrystalline ZrO2. Journal of materials science. 2005, 40(19), 5265-8.

[19] Kirkegaard P; Eldrup M; Mogensen OE; Pedersen NJ. Program system for analysing positron lifetime spectra and angular correlation curves. *Computer Physics Communications,* 1981, 23(3), 307-35.

[20] Chandler H, editor. Hardness testing. ASM international; 1999.

[21] Lutterotti L; Bortolotti M; Ischia G; Lonardelli I; Wenk HR. Rietveld texture analysis from diffraction images. Z. Kristallogr. *Suppl.* 2007, 26, 125-30.

[22] Chanda A, De M. X-ray characterization of the microstructure of α-CuTi alloys by Rietveld's method. *Journal of alloys and compounds*, 2000, 313(1-2), 104-14.

[23] Pal H; Chanda A; De M. Characterisation of microstructure of isothermal martensite in Fe–23Ni–3.8 Mn by Rietveld method. *Journal of alloys and compounds*, 1998, 278(1-2), 209-15.

[24] Sahu P; De M; Kajiwara S. Microstructural characterization of stress-induced martensites evolved at low temperature in deformed powders of Fe–Mn–C alloys by the Rietveld method. *Journal of alloys and compounds,* 2002, 346(1-2), 158-69.

[25] Sahu P; Hamada AS; Ghosh RN; Karjalainen LP. X-ray Diffraction Study on Cooling-Rate-Induced γ fcc→ ε hcp Martensitic Transformation in Cast-Homogenized Fe-26Mn-0.14 C Austenitic Steel. *Metallurgical and Materials Transactions A,* 2007, 38(9), 1991-2000.

[26] Sahu P, De M. Microstructural characterization of Fe–Mn–C martensites athermally transformed at low temperature by Rietveld method. *Materials Science and Engineering: A,* 2002, 333(1-2), 10-23.